Molecular Crystals and Liquid Crystals

ISSN: 1542-1406 (Print) 1563-5287 (Online) Journal homepage: http://www.tandfonline.com/loi/gmcl20

Investigation of thermophysical properties of epoxy nanocomposites

A. Buketov, P. Maruschak, O. Sapronov, M. Brailo, O. Leshchenko, L. Bencheikh & A. Menou

To cite this article: A. Buketov, P. Maruschak, O. Sapronov, M. Brailo, O. Leshchenko, L. Bencheikh & A. Menou (2016) Investigation of thermophysical properties of epoxy nanocomposites, Molecular Crystals and Liquid Crystals, 628:1, 167-179, DOI: 10.1080/15421406.2015.1137122

To link to this article: http://dx.doi.org/10.1080/15421406.2015.1137122

MOL. CRYST. LIQ. CRYST.
2016, VOL. 628, 167–179
http://dx.doi.org/10.1080/15421406.2015.1137122

Taylor & Francis
Taylor & Francis Group

Investigation of thermophysical properties of epoxy nanocomposites

A. Buketov[a], P. Maruschak[b], O. Sapronov[a], M. Brailo[a], O. Leshchenko[a], L. Bencheikh[c], and A. Menou[d]

[a]Kherson State Maritime Academy, Ukraine; [b]Ternopil Ivan Pul'uj National Technical University, Ukraine; [c]Office de la Formation Professionnelle et de la Promotion du Travail, OFPPT, Casablanca, Morocco; [d]Office National des Aéroports (ONDA), Académie Mohammed VI, AIAC, Aéroport Casablanca Mohammed V, Nouaceur, Morocco

ABSTRACT

The effect of nano-fillers (carbon carbon nanotubes) on thermophysical properties of epoxy composites is investigated. The curve showing the dependence between the heat resistance of epoxy composite and the content of nanoparticles demonstrates the optimal content of carbon carbon nanotubes, indicating the improved performance characteristics of the material with the above content of carbon carbon nanotubes. To analyze the processes of structure formation and the behavior of composites under the influence of a thermal field, the thermal coefficient of linear expansion of materials is investigated. It is established that the thermal linear expansion coefficient of materials increases with an increase in temperature within different temperature areas under study. Additionally, the thermogravimetric (TGA) and differential thermal (DTA) analysis of the materials were conducted for the investigation of nanocomposites under elevated temperatures. The maximum values of endothermic and exothermic effects in composites depending on their filling are found.

KEYWORDS

composites; thermophysical properties; temperature; filler particles

Introduction

It is known that a spatial network is formed in epoxy composites during polymerization. Within this gird, filler particles of different physical nature and dispersion affect the structural transformation of materials [1, 2]. The selection of ECMs (epoxy composite materials) as study objects is caused by their widespread use in various industries (shipbuilding, car industry, aerospace engineering) [3, 4]. Thus, the choice of an epoxy composite depends primarily on the operating conditions of the obtained materials. In particular, during the development of protective coatings based on epoxy binders, which have found practical application in various industries, the coating properties such as shrinkage, adhesion, physical, mechanical, thermophysical properties are taken into account, as well as the peculiarities of their production and application technology [5, 6].

Structural ECMs are composites with high adhesion to the reinforcing fiber, low shrinkage and cohesive strength in the hardened state. The use of monomers and oligomers with

CONTACT P. Maruschak maruschak.tu.edu@gmail.com
Color versions of one or more of the figures in the article can be found online at www.tandfonline.com/gmcl.

branched functional groups provides an advanced cross-linking of components and heat resistance of ECMs [7, 8]. At the same time, the matrix brittleness increases under a dense cross-linking, which, in particular, causes the nucleation of cracks in reinforced laminated plastics. It is known from literature [9,10] that the nucleation and propagation of cracks in the polymer matrix is a primary mode of the ECM failure. So, physical and chemical solutions aimed at increasing the level of plastic deformation of the epoxy matrix, strength and other operational and functional characteristics, are critical. Also important and topical are the problems of optimizing the composition and super-molecular structure of the epoxy matrix, which are associated with the improved physical and mechanical characteristics of ECMs [11, 12]. However, despite significant advancements in polymer materials science, not enough attention is paid today to the processes of structure formation and interaction between components in the filled systems. To-date, the interaction between the filler particles and segments/groups of macromolecules of the binder can be examined using modern spectral studies. In particular, the methods of infrared (IR) spectroscopy and differential-thermal analysis (DTA) are among the main methods for studying variations in the structure of polymers under the effect of external factors [14–16]. Further research is also required in the field of structural changes in protective coatings with dispersed additives, including nanofillers, at elevated temperatures.

The purpose of this work is to investigate the effect of the nanofiller content on the structural transformation processes during the cross-linking and thermal destruction of epoxy composites.

Materials and research technique

Diane epoxy oligomer ED-20 (GOST 10587–84) was chosen as the main component of the binder during the formation of a nanocomposite material (NCM).

The polyethylenamine (PEPA) hardener (6-05-241-202-78 TU) was used for the cross-linking of epoxy compositions, which allows hardening the materials at room temperatures. It is known [2] that the PEPA is a low molecular substance, which consists of the following interrelated components: $[-CH_2-CH_2-NH-]_n$. CMs were cross-linked by introducing the hardener into the composition under the stoichiometry ratio between the components and the content (pts. wt.) ED-20: PEPA us 100: 10.

Carbon carbon nanotubes (NTs) l = 500 nm (length) and d = 5 nm (diameter) were used as fillers during the experimental studies. Moreover, epoxy CMs filled with NTs were formed using a technology that involves the ultrasound dispersion of compositions and maintaining the pre-set temperature and time mode of hardening.

Epoxy NCMs were formed by the following technology: pre-dosing of the diane epoxy resin ED-20, its heating to a temperature of T = 353 ± 2 K and holding at a given temperature over time τ = 20 ± 0.1 min; dosage of the nanofiller and its introduction into the epoxy oligomer; hydrodynamic combination of oligomer ED-20 and the nanofiller over time τ = 1 ± 0.1 min; ultrasonic treatment (UST) of the composition over time τ = 1.5 ± 0.1 min; cooling of the composition to a room temperature over time τ = 60 ± 5 min; introduction of the PEPA hardener and stirring the composition over time τ = 5 ± 0,1 min. Next the NCM was hardened under the experimentally established mode: the formation of specimens and their holding over time τ = 12,0 ± 0,1 h at T = 293 ± 2 K, heating at the rate of υ = 3 K/min to a temperature of T = 393 ± 2 K, holding over time τ = 2.0 ± 0.05 hours, slow cooling down to a temperature of T = 293 ± 2 C. In order to stabilize the structural processes in the

NCM, the specimens were held in air during the time $\tau = 24$ h at a temperature of T = 293 ± 2 K followed by experimental tests.

The thermal properties of NCMs, including Martens temperature, thermal linear expansion coefficient, thermal stability (DTA and TGA analysis) are investigated, studies of the flow of physical and chemical processes during the structure formation of the NCM are performed by the IR spectral analysis.

Martens temperature of the matrix was determined in accordance with the GOST 21341-75. The research technique consists in determining the temperature, at which the test specimen was heated at a rate of $\upsilon = 3$ K/min under a constant bending loading of $F = 5 \pm 0.5$ MPa, due to which it deformed by a given value ($h = 6$ mm).

The thermal coefficient of linear expansion (TCLE) of materials was calculated based on the curve showing the dependence between the relative strain and the temperature, by means of approximating this dependence by the exponential function. The relative strain was determined by changes in the length of the specimen while increasing the temperature to the stationary conditions (GOST 15173-70). The dimensions of test specimens were $65 \times 7 \times 7$ mm, the non-parallelism of the polished ends was not more than 0.02 mm. Prior to the investigation, the length of the specimen was measured with the accuracy of ± 0.01 mm. The rate of increase in temperature was $\upsilon = 2$ K/min.

The deviation of values during testing the thermophysical properties of CMs (Martens temperature, TCLE) was 4 … 6% of the nominal value.

To study the influence of the nanofiller nature on the thermal transformations in composites, the method of thermogravimetric (TGA) and differential thermal analysis (DTA) was used, and derivatograph "Thermoscan-2" was applied. The investigations were conducted in the temperature range of $\Delta T = 298$ … 873 K, using quartz crucibles for specimens with the volume of $V = 0.5$ cm^3. During the investigation, the rate of increase in temperature was $\upsilon = 5$ K/min, moreover, the reference substance was Al_2O_3 ($m = 0.5$ g), the weighted quantity of the test specimen was $m = 0.3$ g. The error of determining the temperature was $\Delta T = \pm 1$ K. The accuracy of determining thermal effects was 3 J/g. The accuracy of determining variations in the specimen weight was $\Delta m = 0.02$ g

To determine the nature of the chemical bonds that occur during the formation of the NCM structure, the IR spectroscopy was used. The analysis of infrared spectra was performed by the Lambert-Beer law, taking into account the intensity of passage (%) and half-width (b) of the absorption bands in the spectra of materials. The IR-spectra were deciphered using the techniques provided in [3, 4]. The IR-spectra were recorded on spectrophotometer "IRAffinity-1" (Japan) in the field of wave numbers $\nu = 400$ … 4000 cm^{-1} by a single-beam method in the reflected light. The wavelength scanning by wave numbers $\lambda^{-1} = \nu$ was performed on the diagram within 225 mm in the range of selected frequencies. Wave numbers, the intensity of passage, half-width and area of the absorption band were determined using a computer program IRsolution. The error of determining the wave number was $\nu = \pm 0.01$ cm^{-1}, and the error of determining the peak location was $\nu = \pm 0.125$ cm^{-1}. The photometric accuracy was ± 0,2% in case of a programmed control of a slit and the duration of integration $t = 10$ s. The integration step was $\Delta\lambda = 4$ cm^{-1}. The IR-spectral analysis of nanocomposites was performed with the optimal content of nanoparticles at different stages of thermal degradation. The material was crushed, dried at a temperature of T = 373 K ± 2 during $t = 20$ min, stirred in an agate mortar with the KBr powder, and then specimens were formed on a hydraulic press with loading of $\sigma = 20$ MPa in the following proportion: study material −1 mg, KBr −300 mg.

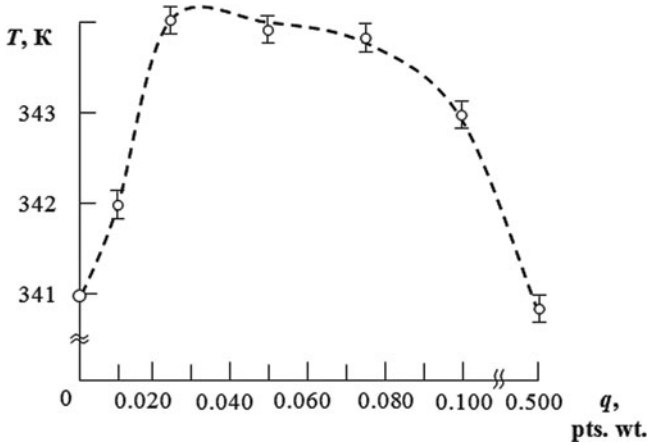

Figure 1. The drawing of the specimen, the position of the PZTs is schematically described.

Investigation results and their discussion

During the formation of protective coatings based on epoxy binders, the value of heat resistance of the material is important. Previous studies have shown [5–7] that heat resistance of the modified epoxy matrix is $T = 341$ K (Fig. 1). Introducing the NT content of $q = 0.010$ pts. wt. leads to an increase in the values of heat resistance to $T = 342$ K. Further increase in the NT content impairs thermophysical properties of NCMs. In particular, the NT content being $q = 0.025$ … 0.075 pts. wt., the heat resistance of NCMs is $T = 341$ …342 K.

It should be noted that the values of Martens temperature of composites differ insignificantly from the matrix indices ($\Delta T = \pm 3$ K). Next, the behavior of composites was investigated under the influence of the thermal field (TCLE). The investigation was performed in the temperature range of $T = 303$ …473 K (Table 1).

An expansion of NCMs, which is accompanied by an increase in the TCLE of the developed materials with an increase in temperature, is established experimentally. In particular, the lowest thermal coefficient of linear expansion ($\alpha = 5{,}54\times10^{-5}$ K) is established within the temperature range of $\Delta T = 303$ …323 K for the CMs filled with the NT content of $q = 0.025$ …0.050 pts. wt. Within the temperature range of $\Delta T = 303$ …373 K, the lowest TCLE ($\alpha = 5.24\times10^{-5}$ K) is characteristic of CMs filled with the NT content of $q = 0.075$ pts. wt. Within the temperature range of $\Delta T = 303$ …423 K, the lowest TCLE ($\alpha = 8.11\times10^{-5}$ K) is characteristic of CMs filled with the NT content of $q = 0.075$ pts. wt. It should be noted that the lowest value of TCLE within the range of elevated temperatures $\Delta T = 303$ …473 K

Table 1. Thermal coefficient of linear expansion (TCLE) of NCMs within different experimental temperature ranges.

		Thermal coefficient of linear expansion, α, K^{-1} Temperature range, ΔT, K			
N	NT content, q, pts. wt.	303 …323	303 …373	303 …423	303 …473
1	0.010	4.76	5.90	9.26	1.07×10^{-4}
2	0.025	5.54	6.10	8.18	1.04×10^{-4}
3	0.050	5.54	6.10	8.31	1.04×10^{-4}
4	0.075	6.38	5.24	8.11	1.05×10^{-4}
5	0.100	5.50	5.39	8.12	1.06×10^{-4}
6	0.500	5.50	5.39	8.12	1.06×10^{-4}

Table 2. Heat resistance of CMs filled with NT.

NT content, q, pts. wt.	T_0, K	T_5, K	T_{10}, K	T_{20}, K	$T_к$, K	ε_m, %
–	593	616	625	641	723	60.0
0.010	597	605	621	634	723	63.3
0.025	609	614	625	640	730	61.6
0.050	609	616	622	638	735	58.6
0.075	600	613	622	636	734	60.6
0.100	603	609	623	639	711	93.3
0.500	607	618	622	633	719	76.6

is characteristic of CMs filled with the NT content of $q = 0.025 \ldots 0.050$ pts. wt. At the same time it is established that the values of TCLE within the range of elevated temperatures differ insignificantly for the composites with different filler content ($\Delta\alpha = \pm 0.03 \times 10^{-4}$ K), indicating the uniformity of physical and chemical processes during the cross-linking of NCMs. In addition, it should be noted that in accordance with investigation results obtained within different temperature ranges, the minimal values of TCLE were obtained for different filler contents in the CMs. In particular, within the temperature of $\Delta T = 303 \ldots 323$ K and $\Delta T = 423 \ldots 473$ K, it is appropriate to use the CM with the NT content of $q = 0.025 \ldots 0.050$ pts. wt., and during the CM operation within the temperature range of $\Delta T = 323 \ldots 423$ K it is appropriate to use the CM with the NT content of $q = 0.075$ pts. wt.

Special attention should be paid to the results of the investigation into the NCM shrinkage, which does not exceed 1.0 …1.4 % for all the specimens investigated. This allows the application of coatings to the long-length surfaces of complex profile.

Special attention is currently given to the materials exposed to high temperatures. Therefore, the behavior of the developed materials at high temperatures was investigated additionally, using the thermogravimetric (TGA) and differential-thermal (DTA) analysis (Fig. 2, a-f).

The lack of weight loss in materials (Fig. 2, TGA-curve) is established within the temperature range of $\Delta T = 303 \ldots 609$ K, which gives an indirect testimony to the stability of physical and chemical links during an increase in temperature (Table 2). Based on the TGA results the temperature is established, at which the destruction of the CMs filled with nanoparticles begins. The matrix is characterized by the lowest value of temperature ($T = 593$ K), at which the initial stage of destruction begins, indicating the unstable physical and chemical links and significant content of the sol-fraction in it. Detailed analysis of the TGA- and DTA-curves of the epoxy matrix is presented in [6].

It is proved (Table 2) that the beginning of the NCM destruction was observed within the temperature range of $\Delta T = 597 \ldots 609$ K, which exceeds by $\Delta T = 4 \ldots 16$ K the temperature of the weight loss start relative to the matrix. In other words, filling a CM with the NT particles causes an increase in the degree of cross-linking, and, therefore, an increase in the gel-fraction content in the developed materials. So, we can state that for the studied NCMs, the beginning of destruction was observed at $T_0 = 597 \ldots 609$ K, and the end of the process – at $T_к = 711 \ldots 734$ K. The lowest relative weight loss, which is $\varepsilon_m = 58.6$ %, is typical of CMs with the NT content of $q = 0.050$ pts. wt. (Table 2). This testifies to a smaller amount of destroyed physical and chemical links as compared to other NCMs and, thus, to an increased heat resistance of the developed material.

Notice: T_0 is the initial temperature of weight loss (beginning of destruction); T_5, T_{10}, T_{20} is the weight loss temperature (5 %, 10 %, 20 %); $T_к$ is the final temperature of weight loss (end of destruction); ε_m is the relative loss of weight.

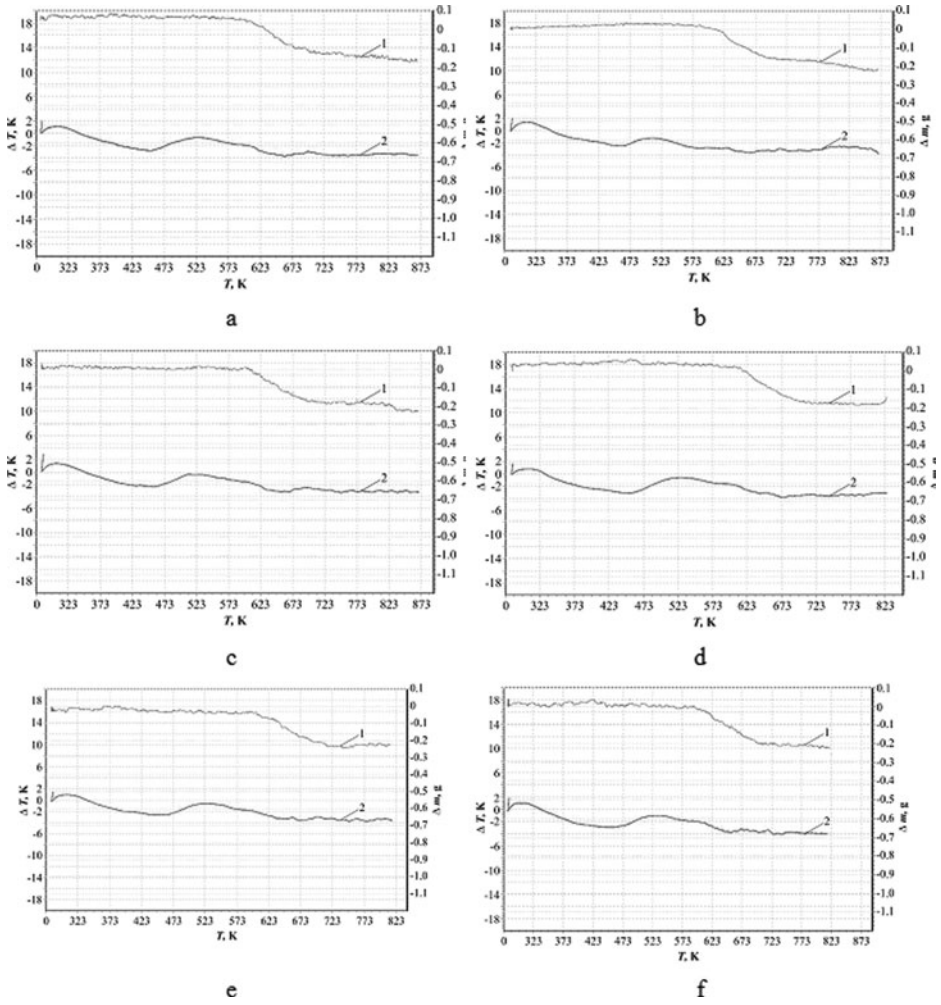

Figure 2. Results of thermogravimetric (1) and differential-thermal (2) analysis for CMs with the NT content of: a) 0.010 pts. wt.; b) 0.025 pts. wt.; c) 0.050 pts. wt.; d) 0.075 pts. wt.; e) 0.100 pts. wt.; f) 0.500 pts. wt.

In general, while analyzing the TGA curve (Fig. 2, a-f), we can state that the thermal destruction takes place in three stages:

- stage one (initial destruction $\Delta T = 593 \ldots 609$ K);
- stage two (intensive destruction $\Delta T = 616 \ldots 641$ K), at which the intensive loss of weight was observed;
- stage three (final destruciton $\Delta T = 723 \ldots 734$ K), at which occurs the emission of the main part of gas-like products, such as carbon oxides and dioxides, etc. In this case, the highest temperature ($T_к = 730 \ldots 735$ K), at which the final destruction occurs, is typical of the CMs with the NT content of $q = 0.025 \ldots 0.075$ pts. wt. (Table. 2).

The exothermal effect (for all the NCMSs investigated) was found experimentally (on the DTA curve) within the area of low temperatures $\Delta T = 293 \ldots 320$ K (Fig. 2). The appearance of this effect was believed to indicate the moisture removal in the CMs investigated. The exothermal effects within the temperature range of $\Delta T = 448 \ldots 671$ K were found additionally (Table. 3). Moreover, the maximal value of the exoeffect peak temperature ($T_{max} = 534$ K) was found for the material with the NT particles content of $q = 0.050$ pts. wt. In the process

Table 3. Temperature intervals of exoeffects of nanocomposites according to DTA.

NT content, q, pts. wt.	Temperature intervals of exoeffects				Maximal value of the exoeffect peak temperature, T_{max}, K
	T_n, K	T_κ', K	ΔT_1, K	ΔT_2, K	
–	460	659	472	3.05	518
0.010	454	660	479	3.17	526
0.025	454	639	458	3.49	508
0.050	454	659	478	1.00	534
0.075	460	663	476	3.39	532
0.100	453	671	491	3.16	526
0.500	448	653	478	1.00	531

of the experimental investigations it was shown (Table 3) that a shift of the exothermal effect peak to the region of high temperatures indicates the improvement of the thermophysical properties of the developed materials under the effect of a thermal field.

Notice: T_n is the initial temperature of exoeffect; T_κ' is the final temperature of exoeffect; ΔT_1 is the temperature interval of exoeffect; ΔT_2 is the temperature difference between a specimen, in which transformations take place, and the reference specimen, in which there are no transformations.

At the same time, we should point out that the greatest value of the temperature interval of the exothermal effect was found for the CM with the NT content of $q = 0.050$ pts. wt. ($\Delta T_1 = 478$ K), which indicates the stability of physical and chemical links and, therefore, the maximal heat resistance of the NCM.

For a more detailed investigation of processes, which occur at different stages of thermal destruction, the performance of the DTA and TGA analyses is not sufficient. Therefore, in order to establish the regularities in the physical and chemical processes that occur in NCMs, the IR-spectral analysis of the obtained nanocomposites at different stages of thermal destruction was performed. Based on the results of the experimental investigations it was established that the maximal values of thermophysical properties are typical of the composites with the NT content of $q = 0.050$ pts. wt. Therefore, it was important to perform the IR-spectral analysis of the nanocomposite (with the NT content of $q = 0.050$ pts. wt.) at the initial (T_0) and final temperature of the weight loss (T_κ) (Fig. 3, curve 1).

Investigations of the processes that take place at the initial (T_n) and final temperature (T_κ'), and the maximum value of the exothermal effect (T_{max}) were conducted as well (Fig. 3, curve 2).

At the initial stage, the physical and chemical links that occurred during the cross-linking of the epoxy composite with the NT content of $q = 0.050$ pts. wt. were investigated (control specimen). The analysis of the IR-spectrum of the composite with the NT content of $q = 0.050$ pts. wt. allowed finding absorption bands within the range of wave numbers $\nu = 420.48 \ldots 567.07$ cm^{-1}, which corresponds to vibrations of –CH_2-groups and para benzene (Fig. 4, a, Table 4). The absorption band at wave number $\nu = 837.11$cm^{-1} corresponds to the pendular –NH–, –CH–, valence –C–C– vibrations of the initial CH_2–NH_2, CH–NH_2 amine group and the epoxy cycle. Absorption bands $\nu = 736.81 \ldots 767.67$ cm^{-1} correspond to pendular vibrations –CH–, –NM– groups and the initial amine groups –NH_2, CH_2–NH_2. We should note the availability of absorption bands at wave number $\nu = 1122.57 \ldots 1188.15$ cm^{-1}, which testify to valence vibrations of –C–C–, –C–N– and –C–O–groups, as well as the primary –CH_2–NH_2– and secondary –CH_2–NH–CH_2 amine groups. An absorption band at wave number $\nu = 1261.45$ cm^{-1} was found as well, which indicates deformation vibrations

Table 4. Characteristic and intensity parameters at different stages of thermal degradation by IR spectral analysis.

Characteristics		IR-spectrum obtained at different stages of thermal destruction (NT content of q = 0.050 pts. wt.)																	
		0.050			0.050 (T_0)			0.050 ($T_к$)			0.050 (T_n)			0.050 (T_{max})			0.050 ($T_к$')		
Group	ν, cm^{-1}	T, %	*b*, cm^{-1}	*S*, %	T, %	*b*, cm^{-1}	*S*, %	T, %	*b*, cm^{-1}	*S*, %	T, %	*b*, cm^{-1}	*S*, %	T, %	*b*, cm^{-1}	*S*, %	T, %	*b*, cm^{-1}	*S*, %
$-CH_2-$group	420.48	32.2	14.1	14.8	–	–	–	–	–	–	15.3	4.4	7.2	15.3	4.4	7.2	5.2	14.4	6.6
$-CH_2-$group	428.20	–	–	–	17.1	9.9	5.6	–	–	–	–	–	–	–	–	–	–	–	–
$-CH_2-$group	474.49	–	–	–	–	–	–	18.8	14.3	11.1	–	–	–	–	–	–	–	–	–
$-CH_2-$ group, para benzene	567.07	28.1	59.2	57.3	–	–	–	–	–	–	–	–	–	–	–	–	–	–	–
$-CH_2-$group, para benzene	578.64	–	–	–	15.8	76.6	52.1	–	–	–	–	–	–	–	–	–	–	–	–
–NH–, –CH– pendular vibrations, initial amine: $-NH_2$; CH_2-NH_2	732.95	–	–	–	–	–	–	–	–	–	19.8	10.8	9.9	19.8	10.8	9.9	–	–	–
–NH–, –CH– pendular vibrations, initial amine groups: $-NH_2$; CH_2-NH_2	736.81	31.4	11.8	15.0	–	–	–	–	–	–	–	–	–	–	–	–	–	–	–
–NH–, –CH– pendular vibrations, initial amine groups: $-NH_2$; CH_2-NH_2	756.10	–	–	–	16.3	16.3	39.2	–	–	–	–	–	–	–	–	–	–	–	–
–NH–, –CH– pendular vibrations, initial amine groups: $-NH_2$; CH_2-NH_2	767.67	30.5	23.7	19.3	–	–	–	–	–	–	–	–	–	–	–	–	–	–	–
–NH–, –CH– pendular vibrations, –C–C– valence vibrations, initial amine groups: CH_2-NH_2, $CH-NH_2$, epoxy cycle	837.11	27.4	62.1	57.9	–	–	–	19.7	32.1	25.7	25.3	26.5	51.7	25.3	26.5	51.7	25.1	26.6	49.5
–NH–, –CH– pendular vibrations, –C–C– valence vibrations, initial amine groups: CH_2-NH_2, $CH-NH_2$, epoxy cycle,	840.96	–	–	–	15.1	20.6	40.2	–	–	–	–	–	–	–	–	–	–	–	–
–C–C–, –C–N–, –C–O– valence vibrations, epoxy cycle	937.40	–	–	–	–	–	–	–	–	–	11.1	22.1	10.2	11.1	22.1	10.3	–	–	–
–C–C–, –C–N–, –C–O– valence vibrations, epoxy cycle	960.55	29.0	19.2	20.6	–	–	–	–	–	–	–	–	–	–	–	–	–	–	–

–OH– deformation vibrations, –C–N–, –C–O– valence vibrations, epoxy cycle, initial amine groups: -NH_2	1261.45	26.0	20.7	43.2	14.4	27.1	23.4	–	–	–	18.8	27.0	25.4	18.8	27.0	25.4	18.0	20.7	24.8
–OH, CH– deformation vibrations, –C–N–, C–O– valence vibrations, tertiary amines: -N–R_2; secondary amine groups: -NH–R, primary amines: -NH_2, epoxy cycle	1315.45	26.8	10.2	19.6	–	–	–	–	–	–	–	–	–	–	–	–	–	–	–
–NH– deformation vibrations, secondary amine groups: -HN–R, CH–HN–CH, CH_2–HN–CH_2	1516.05	23.8	17.5	13.8	13.8	8.9	8.8	–	–	–	15.5	8.8	15.7	15.5	8.8	15.7	15.0	8.7	14.9
–NH– deformation vibrations, –C= C–, –C= N– valence vibrations, -NH_2 primary amines: $–CH_2–NH_2$ amino: –CO–NH_2	1612.49	25.9	14.8	21.9	14.7	9.0	15.8	12.7	11.2	15.1	16.5	11.0	16.2	16.5	11.0	16.2	16.5	11.3	16.2
–C= O–,–C= C–, –C= N– valence vibrations, amino: –CO–NH_2	1666.50	28.9	7.9	10.2	–	–	–	–	–	–	21.1	11.8	5.4	21.1	11.8	5.4	–	–	–
Carbonyl group C–O	1747.51	31.0	8.0	9.6	–	–	–	–	–	–	–	–	–	–	–	–	–	–	–
Valence fluctuations of epoxy group	1886.38	31.3	53.1	30.0	18.0	44.6	20.1	–	–	–	21.2	47.8	22.2	21.0	47.8	22.1	20.8	45.7	21.1
–C≡N– valence vibrations, alkyl group: –C≡C–H	2063.83	32.0	78.9	67.7	–	–	–	–	–	–	–	–	–	–	–	–	–	–	–
–C≡N– valence vibrations	2357.01	19.5	49.7	26.9	2.2	1.1	3.0	2.2	1.1	3.0	2.2	1.1	3.0	2.2	1.1	3.0	2.2	1.1	3.0
–CH– valence vibrations, methyl radical CH_3–C, methylene –CH_2–	2970.38	25.2	59.7	35.9	14.4	40.7	17.7	14.4	11.1	17.7	15.7	13.3	18.3	15.7	13.3	18.3	15.2	12.4	17.9
–CH–, -OH, -NH - valence vibrations, para benzene	3043.67	26.4	36.1	11.1	15.0	22.7	7.7	7.7	12.5	3.2	–	–	–	–	–	–	–	–	–
–OH, -NH– valence vibrations	3498.87	24.8	371.1	13.8	14.4	370.7	12.9	–	–	–	–	–	–	–	–	–	–	–	–

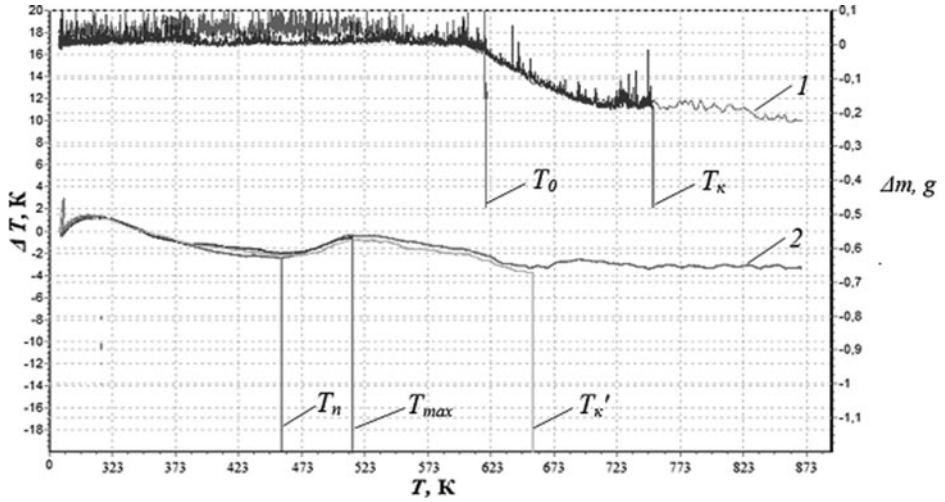

Figure 3. Results of thermogravimetric (1) and differential-thermal (2) analysis during the investigation of thermal destruction of the CMs with the NT content of $q = 0.050$ pts. wt.

of –OH– groups, valence vibrations of –C–O–, –C–N groups, the presence of epoxy groups and the primary amine group $-NH_2$. The presence of absorption bands at wave number $\nu = 1666.50$ cm^{-1} testifies to the existence in the cross-linked nanocomposite of double linkages of valence vibrations –C=C–, –C= N– and –C= O-groups, as well as the amido group $CO-NH_2$. Valence vibrations of the epoxy and –C≡N-groups at wave numbers $\nu = 1886.38 \ldots 2357.01$ cm^{-1} were also found, moreover, the relative value of the peak areas $S = 26.9 \ldots 30{,}0$ % indicates their large number. The characteristic absorption bands, parameters of their intensity, half-width and relative value of the peak area are presented in greater detail in Table 4.

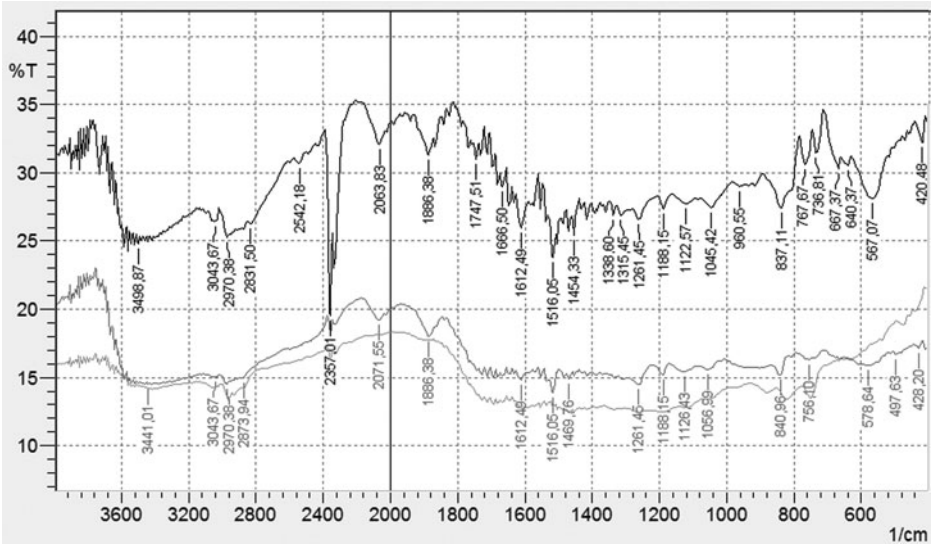

Figure 4. IR-spectrum analysis of the NCM with the NT content of $q = 0.050$ pts. wt.: 1 – spectrum of the cross-linked NCM (control specimen); 2 – NCM spectrum at the initial temperature of the weight loss; 3 – NCM spectrum at the final temperature of the weight loss.

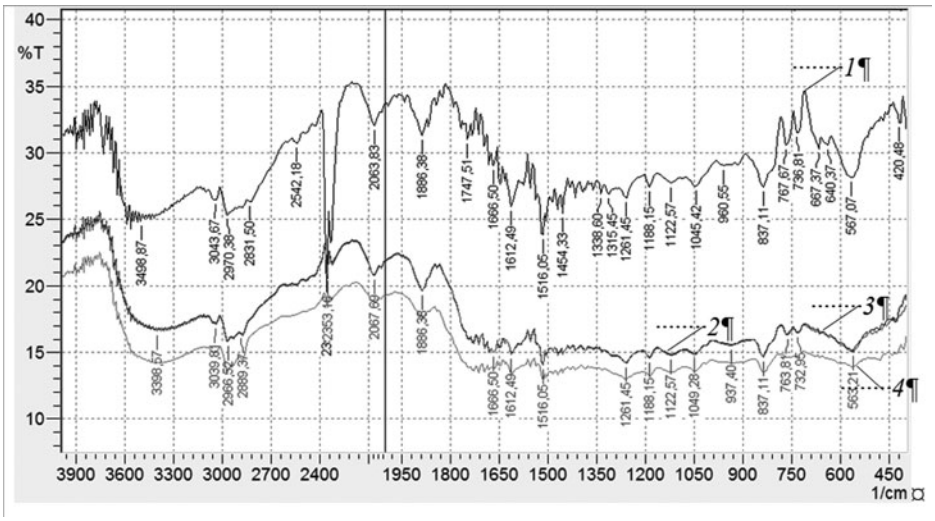

Figure 5. IR-spectrum analysis of the NCM with the NT content of $q = 0.050$ pts. wt.: 1 – spectrum of the cross-linked NCM (control specimen); 2 – NCM spectrum at the initial temperature of exoeffect; 3 – NCM spectrum at the maximum value of exoeffect; 4 – NCM spectrum at the final temperature of exoeffect.

Next we investigated the course of physical and chemical processes at different stages of thermal destruction of nanocomposites. The spectra were recorded gradually with an increase in temperature.

So, as is shown in Fig. 3 (differential-thermal analysis curve), the IR-spectrum analysis was performed to investigate the processes that occur at the initial temperature of the exothermal effect (T_n). The IR-spectrum analysis (Fig. 5, curve 2) allowed finding a decrease in the intensity of passage to $T = 15.3$ %, as well as a decrease in the relative value of the peak area (to $S = 4.4$ %) at wave number $\nu = 420.48$ cm^{-1}. This indicates a beginning of the destruction of $-CH_2$-groups with an increase in temperature. The absence of absorption bands within the range of wave numbers $\nu = 640.37 \ldots 667.37$ cm^{-1} was found additionally, which indicates the destruction of –C–H–links and the alkene group $-C-CH_2$. No less important is a decrease in the intensity of passage, half-width and relative value of the peak area within the range of wave numbers $\nu = 732.95 \ldots 1261.45$ cm^{-1} (Table 4), which indicates a decrease in the mobility of molecular segments of the epoxy oligomer. The absence of absorption bands within the range of wave numbers $\nu = 1315.45 \ldots 1454.33$ cm^{-1} was also found. This indicates the destruction of links -O–H, –C–H–, –C–N–, –C–O–, as well as the secondary and primary amine groups of the epoxy binder. The range of wave numbers $\nu = 1516.05 \ldots 3398.57$ cm^{-1} is characterized by a decreased intensity of passage, half-width and relative value of the peak area, which indicates structural transformations under the effect of temperature. The IR-spectral analysis at the maximal value of the exothermal effect (T_{max}) was not presented in this work, since the obtained spectra coincide (Fig. 5 curve 2, 3), indicating the absence of structural transformations within the temperature range of $T = 454 \ldots 515$ K.

Next we performed the IR-spectrum analysis to investigate the processes that occur at the final temperature of the exothermal effect ($T_к$'). Apart from the above structural transformations, we observed the destruction of -NH–, –CH– groups, as well as the primary amine groups $-NH_2$; CH_2-NH_2 within the range of wave numbers $\nu = 732{,}95 \ldots 1261{,}45$ cm^{-1} with an increase in temperature to $T = 638$ K, which corresponds to the loss of the NCM weight $\Delta m = 20$ %. A decrease in the intensity of passage, half-width and relative value of the peak

area in the range of wave numbers $\nu = 420.48 \ldots 3398.57$ cm^{-1} (Table 4) was also observed, which is typical of an increase in the mobility of molecular segments in the binder during the destructive processes.

At the next stage, we performed the IR-spectrum analysis (Fig. 4, curve 2) at the initial temperature of the weight loss (T_0). It should be noted that in addition to the above mentioned structural transformations, a further decrease in the intensity of passage, half-width and relative value of the peak area (Table 4) was observed. Moreover, a destruction of physical and chemical links was not observed, indicating the thermal stability of the developed nanocomposite. At the final stage, the IR-spectrum analysis of the nanocomposite (Fig. 4, a, curve 3) was performed at the final temperature of the weight loss ($T_к$). It should be noted that at the maximum loss of the NCM weight, the lowest values of the intensity of passage, half-width and relative value of the peak area were observed. A destruction of links within the ranges of wave numbers: $\nu = 428.20 \ldots 750.10$ cm^{-1}, $\nu = 1188.15 \ldots 1469.76$ cm^{-1}, $\nu = 1747.51 \ldots 2071.75$ cm^{-1} was found additionally, which is typical of the third stage of thermal destruction. At the same time, a significant decrease in the amount of hydroxyl groups (a decrease in the relative value of the peak area to $S = 12.9$ %) at wave number $\nu = 3441.01$ cm^{-1} was found, indicating the emission of gas-like products from the NCM.

Conclusions

Based on the conducted research we can state the following:

- it is established that in order to obtain a composite material or a polymer coating with enhanced thermophysical properties, the epoxy binder must be filled with the nanodisperse filler (carbon carbon nanotubes) in the content of $q = 0.025 \ldots 0.075$ pts. wt. per 100 pts. wt. of ED-20 oligomer and 10 pts. wt. of the PEPA hardener. Martens temperature of such a nanocomposite material is $T = 344$ K.
- the behavior of the developed nanocomposites under the effect of the thermal field was investigated. It is established experimentally that within the temperature ranges of $\Delta T = 303 \ldots 323$ K and $\Delta T = 423 \ldots 473$ K, it is appropriate to use the CM with the NT content of $q = 0.025 \ldots 0.050$ pts. wt., and in case of the CM operation within the temperature range of $\Delta T = 323 \ldots 423$ K, it is appropriate to use the CM with the NT content $q = 0.075$ pts. wt.

Using the method of the thermogravimetric and differential-thermal analysis, the heat resistance of the developed nanocomposites was established, which characterizes the final temperature of the weight loss. It is established experimentally that the lowest relative loss of weight, which is $\varepsilon_m = 58.6$ %, characterizes the CM with the NT particles content of $q = 0.050$ pts. wt., moreover, the maximum value of the temperature of the exoeffect peak is $T_{max} = 534$ K.

Based on the IR-spectrum analysis of the developed nanocomposites at different stages of thermal destruction we can state that the process is accompanied by a decrease in the mobility of molecular segments in the binder (as evidenced by a decrease in the intensity of passage, half-width and relative values of the peak area), the emission of gas-like products of destruction, such as water, carbon oxides and dioxides, as well as the destruction of physical and chemical links with a gradual increase in temperature.

References

[1] Yasmin, A., & Daniel, I. M. (2004). *Polymer*, *45*, 8211.

[2] Yang, S.-Y., Lin, W.-N., Huang, Y.-L., Tien, H.-W., Wang, J. Y., Ma, C.-C. M., Li, S.-M., & Wang, Y.-S. (2011). *Carbon*, *49*, 793.
[3] Stukhlyak, P.D., Buketov, A.V., Panin, S.V. et al. (2015). *Physical Mesomechanics*, *18*, 58.
[4] Gao, Z., & Zhao, L. (2015). *Materials and Design*, *66*, 176.
[5] Buketov, A.V., Sapronov, O.O., Brailo, M.V., & Aleksenko, V.L. (2014). *Materials Science*, *49*, 696.
[6] Buketov, A.V., Sapronov, O.O., & Brailo, M.V. (2014). *Strength of Materials*, *46*, 717.
[7] Fu, Y.-X., He, Z.-X., Mo, D.-C., & Lu, S.-S. (2014). *Applied Thermal Engineering*, *66*, 493.
[8] Rashid, E.S.A., Rasyid, M.F.A., Akil, H.M., Ariffin, K., & Kooi, C.C. (2011). *Applied Clay Science*, *52*, 295.
[9] Naik, N.K., Pandya, K.S., Kavala, V.R., Zhang, W., & Koratkar, N.A. (2014). *Polym. Eng. Sci.*, *54*, 2896.
[10] Omar, M.F., Akil, H.M., & Ahmad, Z.A. (2013). *Materials and Design*, *45*, 539.
[11] Lin, W., Zhang, R., & Wong, C. P. (2010). *Journal of Electronic Materials*, *39*, 268.
[12] Wang, S., Tambraparni, M., Qiu, J., Tipton, J., & Dean, D. (2009). *Macromolecules*, *42*, 5251.
[13] Yu, J., Lacy, T.E., Toghiani, H., & Pittman Jr., C.U. (2013). *Composites Part B: Engineering*, *53*, 267.
[14] Moussa, A. A., & Mullen, K. (2011). *Physical Review E*, *83*, 056708/1.
[15] Yang, D. J., Zhang, Q., Chen, G., Yoon, S. F., Ahn, J., Wang, S. G., Zhou, Q., Wang, Q., Li, J. Q. (2002). *Physical Review B*, *66*, 165440/1.
[16] Ganguli, S., Roy, A.K., & Anderson, D.P. (2008). *Carbon*, *46*, 806.